Climate Dynamics (2001) 18: 331–344

M. Drévillon · L. Terray · P. Rogel · C. Cassou

Mid latitude Atlantic SST influence on European winter climate variability in the NCEP Reanalysis

Received: 15 September 2000 / Accepted: 17 April 2001

Abstract Forty one years (1958–1998) of NCEP reanalysis data are used to perform a set of statistical analyses, investigating the interactions between the sea surface temperature (SST), the storm track activity (STA) and the time mean atmospheric circulation in the North Atlantic-Europe (NAE) region. When the atmospheric region of study is restricted to Europe, the singular value decomposition (SVD) lead-lag analysis between seasonal 500 hPa geopotential height (Z500) and SST captures a significant covariance between a summer SST anomaly and a strong winter anticyclonic anomaly over Europe. The summer SST pattern is close to the first empirical orthogonal function (EOF) of SST for the consecutive months J-A-S-O-N. The same analysis, but extending the atmospheric area of interest to the entire NAE region, points out the same signal with a phase shift of one month. A more zonally oriented North-Atlantic-Oscillation-like (NAO) pattern is then found as the SST structure remains practically unchanged. This summer SST anomaly is found to persist through surface heat fluxes exchanges until winter, when it can finally have an impact on the atmospheric circulation. Composites are made from the former SST SVD scores, showing the winter STA and different transient and stationary eddies diagnostics associated with the extreme positive and negative events of the SST anomaly. These suggest that the SST anomaly induces an anomalous stationary wave in winter, creating an initially small anticyclonic anomaly over Europe. Anomalous transient eddies located over northern Europe then strengthen this anomaly and maintain it during winter, thus acting as a positive feedback.

M. Drévillon (✉) · L. Terray · P. Rogel · C. Cassou
Climate Modelling and Global Change Project
CERFACS/SUC URA 1875,
42, Avenue Gustave Coriolis,
31057 Toulouse Cedex, France
E-mail: drevillo@cerfacs.fr

1 Introduction

As the ocean is the slow component of the climate system, it is critical to understand the influence of its interannual variations on the atmosphere to improve seasonal prediction. Tropical sea surface temperature (SST) is of great relevance for climate variability predictability, but the part played by mid-latitude SST is not very well understood yet. One of the major characteristics of Northern Hemisphere mid-latitude winter climate is the occurrence of mean "storm tracks", extending from the regions of high baroclinicity off the eastern coasts of the continents, where the storms develop, then over the Pacific and Atlantic ocean basins and finally reaching the western coasts of the continents. By tracking all winter individual storms characterized by local low pressure centers, Blender et al. (1997) identify three main directions for cyclone tracks (stationary, northeastward and zonal), thus linking the storm track to European weather regimes. This illustrates the central part played by the North Atlantic storm track in the dynamics of the North Atlantic-Europe (hereafter referred to as NAE) region winter climate. The storm track activity (STA) can also be diagnosed by computing the mean winter band pass frequency (about 2–8 day) fluctuations of the 500 hPa geopotential height surface as described in Blackmon (1976).

Schubert et al. (1998) suggest with coupled model studies, that the rising greenhouse forcing can induce an increase of STA over Northern Europe. This local enhancement is linked, following Ulbrich and Christoph (1999), to a northward shift of the centres of action of the North Atlantic Oscillation (NAO). The latter is known to explain a large part of interannual to decadal winter atmospheric variability in the NAE Region (Barnston and Livezey 1987), while seasonal fluctuations in the European climate are better described by the storm track variability. However, variations in the amplitude and position of the Atlantic storm track are closely linked to the NAO. The enhanced westerlies between the two centres of action of the NAO modify the baroclinic wave

guide direction. Principal component analysis shows that negative (positive) phases of the NAO correspond to a zonal (tilted to the northeast) storm track (Lau 1988; Rogers 1990). Nevertheless, using station observations, Rogers (1997) shows that this association may only be indirect, through the Greenland-Scandinavia surface temperature seesaw. Fraedrich et al. (1993) define a European winter climate index based on stations observations of mean sea level pressure (SLP), precipitations and temperature. Composites built from this index describe a strong positive (negative) SLP anomaly over Europe associated with a northward tilted (zonal) tail end of the Atlantic storm track. Branstator (1995) suggests with a GCM study that the storm track organization by certain low frequency circulation patterns can act as a positive feedback maintaining these patterns.

As it deals with low frequency climate fluctuations, this anomalous winter atmospheric circulation may interact with the ocean. It is responsible, through surface fluxes, for the occurrence of a tripole-like SST anomaly (Kushnir 1994). The NAO positive phase corresponds to a mid-latitude positive SST anomaly extending from one side of the basin to the other, a negative anomaly resulting from the enhanced westerlies over the north of the basin, and a sub-tropical negative SST anomaly resulting from trade winds changes. This phenomenon happens at monthly to seasonal scales, but an important part of the decadal variability in the North Atlantic ocean circulation may also be explained by the winter atmospheric stochastic forcing (Frankignoul et al. 1997). The winter atmospheric response to the resulting mid-latitude SST anomalies is ambiguous in the observations, being indistinguishable from the strong internal atmospheric variability which gives rise to the atmospheric stochastic forcing (Frankignoul 1985). Hence the question of an oceanic feedback in the mid-latitudes is still open and the existence of ocean-atmosphere coupled modes in the North-Atlantic Europe region is controversial.

The Atlantic storm track is expected to play a part in the "missing link" providing a way for the SST to feedback upon the atmospheric mean flow. Hoskins and Valdes (1990) propose that the Atlantic storm track is self-maintaining owing to diabatic heating through a positive feedback on baroclinicity, which can be seen as a SST/storm track interaction. Peng et al. (1995) observe the dependence on the background mean state of GCM responses to SST anomalies. Peng and Whitaker (1999) find with idealized models that eddy activity can be one of the main factors modulating these responses. Norris (2000) investigates the link between summer mid-latitude SST and the storm track over the Pacific ocean and finds a positive feedback of the SST through the amount of marine stratiform cloudiness.

In the present study we explore these triangular interactions (SST, storm track and low frequency circulation represented by 500 hPa geopotential height) in the NCEP reanalysis dataset. Bresch and Davies (2000) studied these interactions by applying maximum covariance analysis, also known as singular value decomposition (SVD) analysis, to each possible couple between the three fields, for the 1962–1992 NCEP reanalysis dataset winter seasons. Czaja and Frankignoul (1999) examined the signature of the SST feedback by *lead-lag* SVD analysis between COADS SST and NCEP analysis atmospheric fields. We perform here lead-lag SVD analyses on the NCEP/NCAR reanalysis dataset between SST and 500 hPa geopotential height (hereafter referred to as Z500) over the NAE region. Then composites on different diagnostics of storm track interactions with the mean flow and on stationary wave activity, confirm the assumption of an influence of mid-latitude SST upon the NAE region atmospheric winter circulation.

In Sect. 2 the dataset and method used are described. In Sect. 3 we identify a summer SST anomaly which, as it persists until winter, can have an influence on European winter interannual to decadal atmospheric variability. In Sect. 4 we use composite analysis to assess the non-linearities in the atmospheric response to the SST anomalies, and a mechanism of interaction is proposed. In Sect. 5 we discuss the results and our conclusions.

2 Dataset, diagnostics and statistical methods

The NCEP reanalysis dataset (hereafter referred to as NCEP) described in Kalnay et al. (1996), is used for both atmospheric and SST fields over the 1958–1998 period. A Murakami recursive filter is used to keep back the 2.2–6 day fluctuations z' from the daily NCEP Z500 fields, as recommended in Christoph et al. (1995). The monthly RMS of these fluctuations RMS(z') represents the monthly 500 hPa storm track activity (STA). Surface fluxes are from the COADS dataset (Da Silva and Young 1994).

2.1 Lead-lag SVD analysis

Maximum covariance analysis, also called SVD analysis, is made between NCEP seasonal Z500 and SST. This analysis is based on the singular value decomposition (SVD) of the covariance matrix between the two fields, as described in Bretherton et al. (1992). The first pair of left and right singular vectors obtained are the most strongly covarying spatial patterns of each original field, the strength of the covariance being given by the squared covariance fraction (SCF). For the k-th SVD mode, SCF_k is the ratio between the squared singular value π_k^2 and the sum of all the n squared singular values:

$$SCF_k = \frac{\pi_k^2}{\sum_{l=1}^{n} \pi_l^2} \ .$$

The normalized root-mean-squared covariance (NC_k),

$$NC_k = \sqrt{\frac{\pi_k^2}{(\sum_i \sigma_i^2)(\sum_j \sigma_j^2)}} \ ,$$

where σ_i^2 and σ_j^2 are the variances at the ith grid point in the left field and the jth grid point in the right field, was introduced by Iwasaka and Wallace (1995) and Zhang et al. (1998). It shows the importance of the covariance explained by the SVD mode number k with respect to the maximum possible total squared covariance between the two fields. Both ratios will be presented here as percentages and will help determine the robustness of the covariance signals, together with the correlation between the SVD scores. For a given SVD mode, the latter are defined by the projection of the patterns upon the initial respective fields at each time step, resulting in time series of coefficients for each field.

The statistical significance of the results (covariance and correlation) is tested with a Monte Carlo approach as proposed in Wallace et al. (1992). The atmospheric time series is first randomly scrambled using a moving block bootstrap algorithm as described in Wilks (1997). The length of the blocks is four years, in order to account for the significant one-year-lag autocorrelation in the Z500 data in winter, and the fact that the autocorrelation shows significant regions with positive values up to a 4-year lag. This is consistent with the peak at 2–3 years in the NAO spectra (not shown). It is worth noting here that the results described later remain significant with blocks of 3 or 8 years, as well as when scrambling the SST time series. SVD between SST and the atmospheric field is then computed. The entire operation is performed a hundred times. The significance of the original SVD results is then assessed by comparing with the covariance or correlation values of the hundred randomly scrambled SVDs.

Significance levels for all the other correlation coefficients presented in the text are estimated using the method proposed by Sciremammano (1979). This method accounts for the autocorrelation inherent in the time series to compute the actual number of degrees of freedom before the estimation of significance levels.

The winter (December–January–February, hereafter DJF) synchronously covariant spatial structures of SST and Z500 and of SST and STA obtained by SVD analysis are described in Bresch and Davies (2000), and thus not shown here. The main features are a tripole SST anomaly (warm mid-latitude basin wide anomaly, cold SST anomaly to the north and in the subtropics) covarying with the NAO pattern (enhanced Azores high and deeper Icelandic low). Almost the same tripole is associated with a northern shift in the position of the Atlantic storm track. As the SVD analysis is linear, the opposite sign of the tripole corresponds to a negative NAO phase, and a more southerly position of the storm track, ending in the Bay of Biscay. As reviewed by Frankignoul (1985) the amplitude of the winter atmospheric response to synchronous mid-latitude SST anomalies is weak and not distinguishable from the whole winter atmospheric variability. Hence the first winter covarying mode, explaining about 60% of the covariance between the two fields, gives a good description of the atmospheric forcing, but the possible mid-latitude SST feedback upon the winter atmospheric mean flow is not detected in the few first SVD modes that explain a significant amount of covariance.

SVD *lead-lag* analysis between SST and 500 hPa geopotential height may bring out the signal of this feedback, as shown in Czaja and Frankignoul (1999). If the covariance is strong and significant when the SST field is leading the atmospheric field by more than one month, which is approximately the atmospheric decorrelation time, we can assume that the statistical signature of a SST feedback is detected. This analysis is done here on NCEP (both for atmospheric and SST fields) between SST and Z500.

A second order polynomial trend is first removed from the SST data, and a third order trend from the atmospheric data, so as not to take into account the long term changes into the interannual variability. Each given monthly field is normalized by its standard deviation over the period of study, averaged over the region of study. This filters out the seasonal cycle of variance so that SVD will only capture interannual to decadal variability. The data is weighted by the cosine of the latitude. SVD analysis is then performed on seasonal means. In the present study we will focus on SST leading Z500 by one to four months.

2.2 Composites of transient and stationary eddies

In Sect. 4 composites on a SST index are shown. These are made by selecting a threshold of one standard deviation of the SST time series, giving seven positive events over the positive threshold and five negative events below the negative threshold. This operation selects SST extreme events in both negative and positive phases of the pattern matching the time series. Averaging anomaly fields (for instance of STA) corresponding to these events brings out a negative and a positive composite, showing in this case the STA anomaly linked to respectively negative and positive phases of the SST anomaly. For the lagged composites on the time series, the average is performed on atmospheric anomaly fields systematically lagging the selected extreme events by a given number of months. The statistical significance of these associations is assessed using a student's *t*-test at the 95% level, with 10 degrees of freedom for the difference between positive and negative composite. Sensitivity to the number of events selected for both composites has been tested adding or subtracting a few events. The results are not significantly affected by these changes.

In the following, the prime refers to 2.2–6 day Murakami filtered daily data, and the star refers to deviations from the zonal mean. The low-level poleward transient heat flux $\overline{v'T'}$, where v and T are the meridional wind and the temperature at 700 hPa, characterizes the advection of heat by the transient eddies to the high latitude regions. The meridional and zonal components of the Eliassen-Palm vector **E**, described in Trenberth (1986), Hoskins et al. (1983), and Lau (1988) among others, are provided respectively by the momentum flux of the transient eddies $-\overline{u'v'}$, and $1/2(\overline{v'^2} - \overline{u'^2})$, where u and v are the zonal and meridional wind at 200 hPa. **E** gives a description of the transient eddy forcing upon the local time mean flow. The divergence (curl) of **E** represents the eddy-induced accelerations of the zonal (meridional) wind due to barotropic processes. In the barotropic case, **E** is in the direction of the group velocity of the transient eddies relative to the local time mean flow (Lau 1988; Trenberth 1986). The characteristic shape and horizontal tilt of the eddies can also be determined from the angle of **E** with the zonal direction (see Hoskins et al. 1983). Low level baroclinicity (850 hpa) is estimated through the Eady baroclinic instability growth rate maximum (Lindzen and Farrel 1980; Hoskins and Valdes 1990)

$$\sigma_{BI} = 0.31 f |\partial u/\partial z| N^{-1} \ ,$$

where f is the Coriolis parameter, u the zonal wind, and N the Brunt-Väisälä frequency. Mean NCEP DJF baroclinicity and STA are displayed in Fig. 1a. In the NAE region, the baroclinicity maxima are located over the Gulf Stream current and south east of Greenland, the STA maximum extending downstream of these zones. In Fig. 1b, mean DJF $\overline{v'T'}$ and **E** also indicate the regions of STA maximum showing respectively the mean eddy negative and positive feedbacks. Within the storm track the maximum of $\overline{v'T'}$ acts to reduce the meridional temperature gradient and thus decreases baroclinicity. The divergence of **E** represents the vorticity flux convergence accelerating the jet stream, thus enhancing baroclinicity.

The plumb vector **F**, defined in Plumb (1985) and Fraedrich et al. (1993), is a diagnostic tool for the three-dimensional *stationary wave* activity. **F** is derived from a locally applicable conservation relation for quasi-geostrophic waves on a zonal flow. The zonal $\frac{\sigma}{2f^2}(\phi_x^{*2} - \phi^*\phi_{xx}^*)$ and meridional $\frac{\sigma}{2f^2}(\phi_x^*\phi_y^* - \phi^*\phi_{xy}^*)$ components of **F**, where $\sigma = p/1000$ hPa, are computed here from the monthly zonally asymmetric part of the time mean 500 hpa geopotential $\phi^* = gz^*$. An anomalous divergence (convergence) of the **F** vectors depicts a region of creation (dissipation) of an anomalous stationary wave. **F** is also parallel to the direction of propagation of stationary waves. The mean NCEP DJF **F** vector in Fig. 1d shows the major three sources of stationary wave activity in the Northern Hemisphere (Eastern Asia, Western North Atlantic, North Pacific-Western North America) and the direction of propagation of the wave trains of DJF z^* (Fig. 1c).

3 Covariations between summer SST and winter atmospheric circulation

3.1 A European atmospheric low-frequency variability mode linked to the summer SST anomaly

As shown in Fraedrich et al. (1993), the Atlantic storm track is linked to a strong anticyclonic SLP anomaly over Europe through a poleward deflection of its tail end. The eastern part of the storm track reaches either

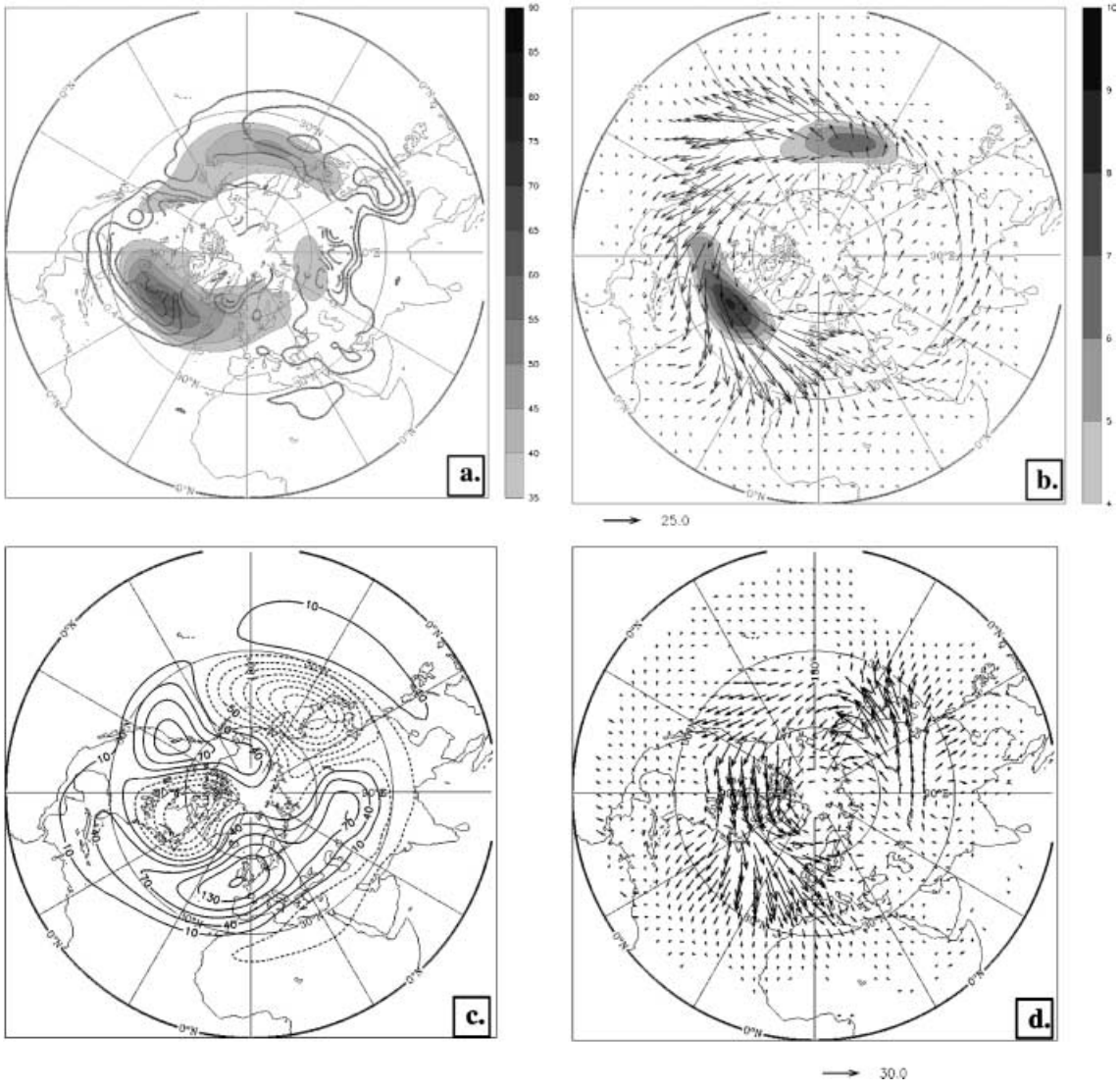

Fig. 1a–d NCEP reanalysis mean winter (DJF) **a** Eady baroclinic instabilities growth rate maximum at 850 hPa σ_{BI} in day^{-1} (*thick contours*) and storm track activity at 500 hPa (*shaded*, *thin contours*) $\overline{z'^2}$ (m), **b** horizontal Eliassen-Palm vector at 200 hPa **E** (m$^2 \cdot$ s^{-2}) and transient eddy meridional heat transport at 700 hPa $\overline{v'T'}$ (m $\cdot$ K $\cdot$ s^{-1}), **c** 500 hPa geopotential height deviation from the zonal mean z^* (m), and **d** Plumb vector **F** (m$^2 \cdot$ s^{-2})

Southern Europe (in the cyclonic anomaly case) or Scandinavia (in the anticyclonic one). With composites on their European winter climate index, they show that a small anticyclonic anomaly over Europe might be first created by an anomalous stationary wave, and then be strengthened and maintained by transient eddies interactions: the initial SLP anomaly shifts the tail end of the storm track to the north which could subsequently positively feedback onto the anticyclonic anomaly to amplify and maintain it. This finding (hereafter referred to as the Fraedrich mechanism) made us focus on European climate, performing a lead-lag SVD analysis between North Atlantic SST and an area of study restricted to Europe for the atmosphere (from 10°W to 50°E, and from 20°N to 7°N). In the following, SVD A refers to this analysis.

Large covariances are found when Z500 leads SST (not shown), but a "feedback signal" (when SST leads Z500) is also detected: a strong and significant covariance between August–September–October (ASO) SST and the next DJF Z500. The latter, hereafter referred to as the summer SST signal, shows a summer SST pattern that can have an influence on the next winter atmosphere. This signal is detected when SST leads by 4 (ASO SST), 3 (September–October–November [SON] SST), 2 (October–November–December [OND] SST), and 1 month (November–December–January [NDJ] SST) the next DJF Z500. The SVD A heterogeneous covariance patterns of ASO SST and DJF Z500 (lag 4) are displayed in Fig. 2a. The atmospheric pattern strongly projects onto the NAO dipole, the anticyclonic anomaly spliting here into a western and an eastern part.

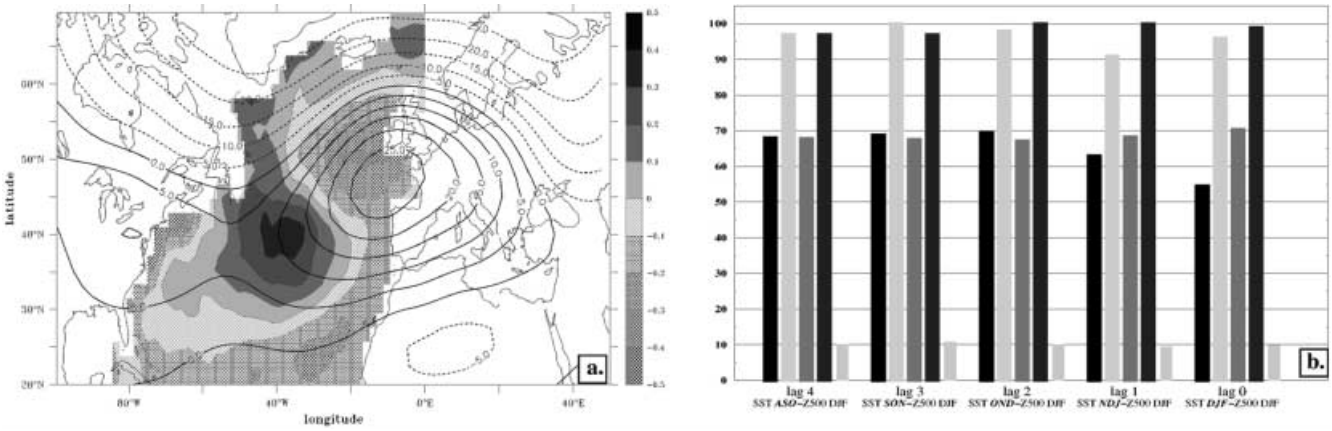

Fig. 2a, b SVD A between North Atlantic SST and Z500 over Europe, **a** covariant patterns of SST (°C) in ASO (*grey levels*) and Z500 (*m*) in DJF (*thick contours*), and **b** for each lag and from left to right: percentages of covariance explained or SCF (*black*), significance level of SCF according to Monte Carlo test (*light grey*), correlation between SST and Z500 SVD scores (*medium grey*), significance level of correlation according to Monte Carlo test (*medium dark grey*), and normalized square covariance (*medium light grey*)

The summer SST pattern, a warm central anomaly circled to the east by a cold anomaly, is also the first SST variability mode in the North Atlantic basin, explaining 37% of SST variance. The latter is obtained by principal component analysis on the consecutive months July, August, September, October and November (J-A-S-O-N), the individual months still being normalized by their standard deviation averaged over the region as described in Section 2.1 (not shown). The SVD A SST pattern slightly changes as winter approaches (from lag 4 to lag 3, 2, and then 1 month), the warm part being advected to the east and the southern cold part to the west with some intensification. At lag 0 the SST influence is not distinguishable from the atmospheric forcing, and thus will not be described here.

In Fig. 2b, a diagram made of five sets (one for each lag, including lag 0) of five columns is displayed. The columns stand respectively from left to right for the squared covariance fraction and its statistical significance, the correlation between the SST and Z500 SVD A scores and its statistical significance and the normalized squared covariance defined in Sect. 2.1. The covariance is significant (over 90%) at every lag, and the mode is explaining 55 to 70% of covariance between Z500 and SST. The correlation between the scores reaches about 70% and is statistically significant (over 95% for each lag). At those particular lags identified as a significant covariance signal, the SVD mode explains 15% to 20% of the Z500 variance and 10 to 15% of the SST variance (not shown). The summer SST signal reaches NC values of about 10%, which is comparable to the results of Iwasaka and Wallace (1995) in their Table 1, for synchronous winter SVD between Z500 and SST. Thus the SVD A analysis captures a significant lagged relationship between natural variability modes of each field. In addition, this relationship is shown to be realistic by performing ASO SST empirical orthogonal functions (EOF) and DJF Z500 EOF. The SST and Z500 first EOF patterns are not shown as they closely resemble the covarying patterns of the first mode of SVD A displayed in Fig. 2a. The first principal components of SST and Z500 are strongly correlated with the respective SVD A scores (0.95 for the Z500 time series and 0.86 for the SST time series, significant at the 99% level). The former are by construction generated independently and have a correlation of 0.4 significant at the 99% level. These results confirm that the summer SST signal of SVD A analysis is not obtained by chance.

Table 1 Correlation coefficients between monthly SST time series extracted from the first principal component of North Atlantic SST for J-A-S-O-N consecutive months displayed in Fig. 3. All coefficients are significant at the 99% level except the one in italics

	A	S	O	N
J	0.89	0.63	0.48	*0.31*
A	1	0.81	0.59	0.44

A second lead-lag SVD analysis is performed, hereafter referred to as SVD B, where the area of study is the entire NAE region for both oceanic (from 85°W to 0°E, and from 20°N to 70°N) and atmospheric (from 100°W to 50°E, and from 20°N to 70°N) fields. The results of SVD B between SST and Z500 are comparable to those of Czaja and Frankignoul (1999) regarding the following three points (not shown): the largest covariances are found when Z500 leads SST; a feedback signal is detected between DJF SST and the next February–March–April (FMA) Z500; the summer SST signal described previously is also found in SVD B analysis, but this time significantly linking July–August–September (JAS) SST to NDJ Z500 (earlier in the year than in SVD A but with same lag 4). The respective covarying patterns of SST and Z500 are not shown as they closely resemble those of SVD A analysis (Fig. 2a). It is worth noting here that the SVD A analysis yields a broader and stronger anticyclonic anomaly over Europe, and a SST pattern consistent

with a propagation to the east of the SVD B one. The SST anomalies SVD scores of SVD A and SVD B are correlated up to 0.82, while Z500 SVD A and B scores correlation is 0.62 which is significant at the 99% level. When SST leads NDJ European area Z500 by 4, 3, 2 or 1 month, the SVD B patterns are found to covary significantly but display lower SCF (50 to 65%) and correlations (60 to 75%). At every lag NC reaches 10%, as in SVD A results.

In Czaja and Frankignoul (1999) there was a gap in the statistical significance at lag 2, that is in their case between ASO SST and OND Z500. Their computations have been performed with series of monthly anomalies instead of seasonal means, thus allowing intraseasonal changes in the atmosphere, which may explain this difference. They also used a different dataset (NCEP analysis data for the atmosphere and SST COADS dataset) which was probably less reliable than the NCEP reanalysis. The period chosen for their study is different (1952–1992) but tests have been made to make sure that a change of a few years in the period does not alter significantly the results, neither does a small shift in the spatial region selected. However, these findings all together confirm the robustness of the signals.

The comparison between SVD B results and JAS SST EOF and NDJ Z500 EOF shows that the first principal component of each field is strongly correlated to the respective SVD B scores. The correlation between the atmospheric and oceanic first principal components is significant at the 99% level, and reaches 0.4. Hence the relationship between a summer SST variability mode and the next winter NAO is robust with respect to a change in the SVD analysis regions of study. The signal is stronger when considering a strictly European atmospheric variability mode rather than the classical NAO spatial structure (extending over the whole NAE region).

3.2 Persistence of the North Atlantic summer SST anomaly

The SST SVD scores from the SST/Z500 SVD A summer signal are well correlated with the first principal component of North Atlantic SST for the consecutive normalized months J-A-S-O-N (Fig. 3). Each black dot symbolizes a month in the J-A-S-O-N sequence. If the principal component changes sign during one J-A-S-O-N period it suggests that the anomaly does not persist through that period. The persistence of this mode is approximately four months, since the monthly time series of August and November extracted from the J-A-S-O-N series are still correlated up to 0.44 (Table 1), which is significant at the 99% level.

These results support the hypothesis that the response to this summer SST signal is due to the persistence of the SST anomaly from summer until winter, when it can finally have an impact on the NAE atmospheric circulation. To investigate this hypothesis, one must find out which mechanisms can help to create this SST anomaly in summer and maintain it until winter. The linear regression of COADS total surface heat fluxes on the period 1958–1989 built from the summer SST anomaly time series for lag 4, 3, 1, and 0 is displayed in Fig. 4. These regressions are comparable to NCEP fluxes regressions for the same period, and for the 1958–1998 period. Negative fluxes mean that the ocean is losing heat to the atmosphere. Lag 2 regression is not shown as it is very close to lag 3 (Fig. 4b) and 1 (Fig. 4c).Immediately after the summer SST anomaly has been generated (ASO), the surface heat fluxes tend to damp the south west region of its central part (Fig. 4a). In Fig. 4b the heat fluxes reverse sign over the SST anomaly, thus becoming likely to maintain it rather than damp it, with negative (positive) heat flux over the cold (warm) parts of the anomaly. Figure 4c exhibits large significant re-

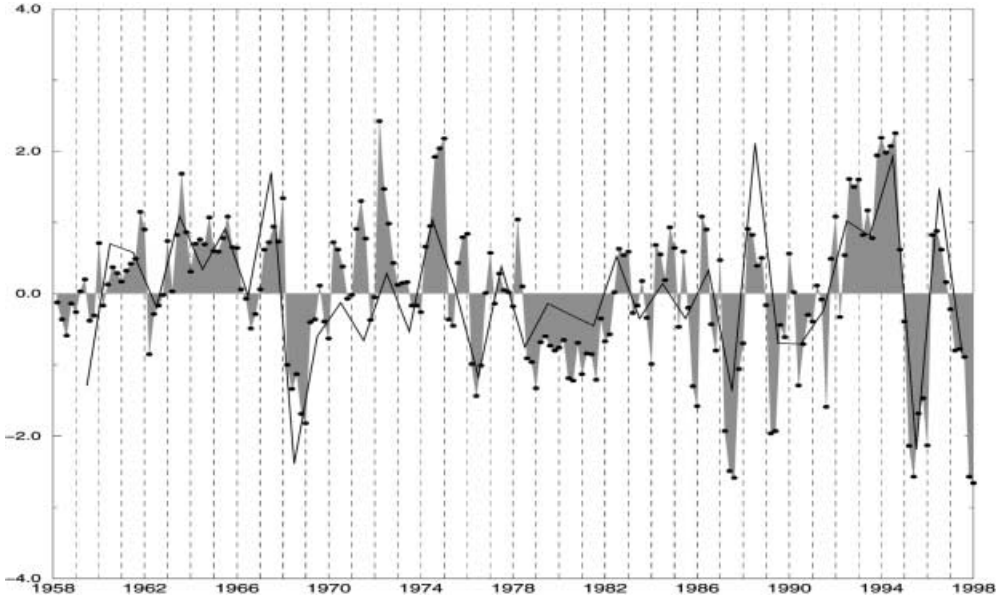

Fig. 3 First principal component of SST for the series of consecutive months J-A-S-O-N (*shaded*), each *black dot* is a month in the series. SVD A (between SST in ASO and Z500 in DJF) scores of SST (*black line*). Composites of Figs. 5 to 8 have been built on this SST index. Both time series have a standard deviation of 1

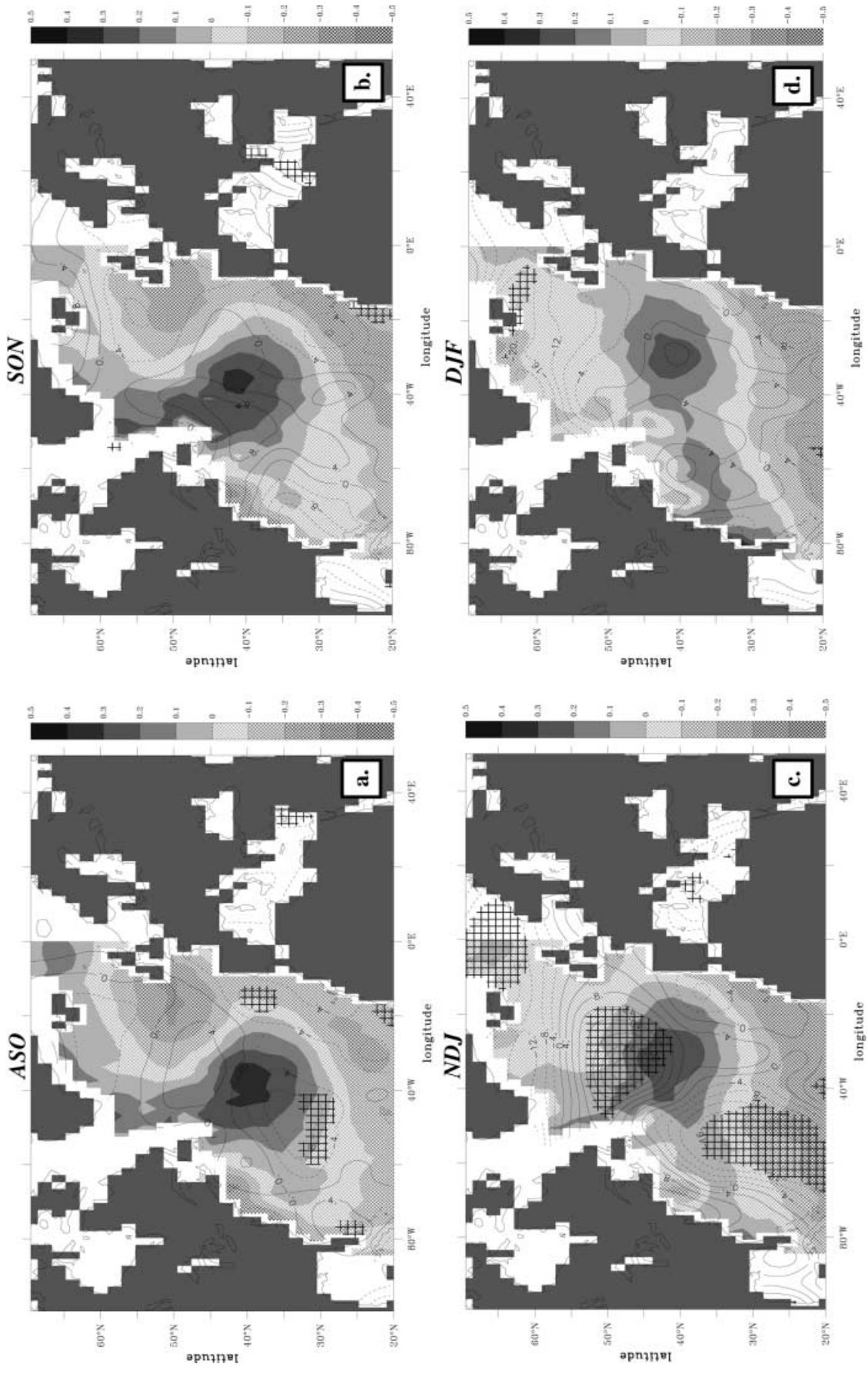

Fig. 4a–d Regression of total surface heat fluxes in W/m^2 (contours) overlaying the corresponding SST SVD anomaly in °C (*grey levels*). **a** Regression of September heat fluxes on SST SVD scores SST/Z500 lag 4 (ASO/DJF), **b** regression of October heat fluxes on SST SVD scores SST/Z500 lag 3 (SON/DJF), **c** regression of December heat fluxes on SST SVD scores SST/Z500 lag 1 (NDJ/DJF), and **d** regression of January heat fluxes on SST SVD scores SST/Z500 lag 0 (DJF/DJF). Statistically significant regions according to a *t* test at the 95% level are gridded

gions which suggest that the interaction with the atmosphere maintains the SST anomaly and may drive the warm (cold) part to the east (west). Advective phenomena may also play a part in this shift. Finally at lag 0 (January) the heat fluxes tend to drive the SST into a tripole anomaly, which is the typical winter situation. Total heat fluxes thus are likely to allow the maintenance of the summer SST anomaly until December. Latent heat fluxes play the major part in the persistence of the latter, while solar heat fluxes may initially create it (not shown).

4 Winter atmospheric state following the SST anomaly occurrences

The summer SST anomaly SVD A scores (SST in ASO covarying with DJF Z500) displayed in Fig. 3 provide an SST index that is used to build composites, as defined in Sect. 2, of the different atmospheric flow diagnostics defined in Sect. 2.2, and for all seasonal means from ASO to DJF. These lagged composites show the atmospheric changes that can be significantly linked to the persisting summer SST anomaly as fall and winter go along, and as the maximum phase of the seasonal cycle of the NAE region STA (DJF) is getting closer. This method helps us determine to what extent each factor of the Fraedrich mechanism (transient eddies, stationary wave activity) is responding to the summer SST anomaly. Only the peak season (DJF) composites are shown here, as they show the most significant response.

4.1 Composites of transient eddy activity

The DJF STA and σ_{BI} responses to a cold phase (cold anomaly in the centre circled to the east by a warm anomaly) and warm phase of the summer SST anomaly are displayed in Fig. 5. In the positive composites in DJF, an enhancement of STA localized in Northern Europe is associated with a reduction of STA over south-western Europe. This suggests that the warm phases of the summer SST anomaly are associated with a northeastward shift of the Atlantic storm track. This response is consistent with the SVD A results in Sect. 3.1 as the increase of STA is localized in the region of maximum pressure gradient in Fig. 2a, and close to the STA pattern found by SVD A analysis between SST and STA (not shown). The difference between the positive and the negative composite show the regions (over Europe and over the Gulf Stream) where the STA response to the summer SST anomaly is significant. The latter is asymmetrical since the negative composite structure is extended over the whole NAE region, with a significant region over the Gulf Stream, whereas the positive composite significant regions are strictly localized over Europe.

Negative (positive) composites of Eady growth rate σ_{BI} in Fig. 5d (e) display the baroclinicity maximum region responsible for an enhancement of STA over Southern (Northern) Europe. The difference between the positive and negative composites shows a strengthening of the baroclinicity in the northern part of the North Atlantic basin associated with a decrease over most Europe and a latitudinal band between 20°N and 40°N. In the negative composite, the baroclinicity maximum region is in the Gulf of Mexico and Gulf Stream region, whereas in the positive ones it is more to the southeast of Greenland. These responses are consistent with that of STA, since the negative and positive composite STA anomalies are found downstream of the respective composite baroclinicity anomaly. These results again support the idea that the atmospheric response to this SST anomaly is asymmetrical.

The local strengthening of the jet stream, and thus maintenance of the baroclinicity linked to the SST anomaly is displayed in Fig. 6, with composites of the horizontal Eliassen Palm vector **E**. A strong divergence over the North Atlantic basin can be observed in the negative composite, together with easterly and convergent **E** vectors over Scandinavia. The former is associated with a local acceleration of the jet stream, in contrast with the latter which is characteristic of a deceleration. The positive composites show an acceleration of the jet stream by the eddies over Scandinavia and a deceleration over the centre of the North Atlantic ocean basin. This response can be found clearly in the difference between the positive and negative composites, with significant parts over Northern Europe and North Africa. These results are still consistent with the other composites as they show that a positive feedback is possible in the region of higher STA. Eddy vorticity flux convergence can thus play a role in driving the anomalous Z500 anticyclonic circulation.

The same type of influence is found in the composites of poleward transient heat flux $\overline{v'T'}$ as well as in the difference between positive and negative composites. More heat is transported to the north of Europe by the transient eddies in the positive composites, whereas in the negative composites there is less heating in this region concurrent with a significant transport of heat over the Atlantic ocean and off the North American coasts. This transient eddy heat flux is a characterization of the tendency of the storms to decrease the baroclinicity which first made them grow. On the contrary, the Eliassen Palm vector represents the tendency of the eddies to strengthen the latter by conveying momentum flux into the jet stream. The net effect results in a positive feedback of the storms onto the mean flow.

Hence these composites all together show that there is an influence of the summer SST anomaly over the North Atlantic storm track and its interactions with the mean atmospheric circulation. This influence is significant in winter, and helps to maintain a strong Z500 anticyclonic anomaly over Europe in the case of a warm phase of the SST anomaly. As for the cold phase, it brings more storms over the North Atlantic ocean in the direction of the Mediterranean Sea.

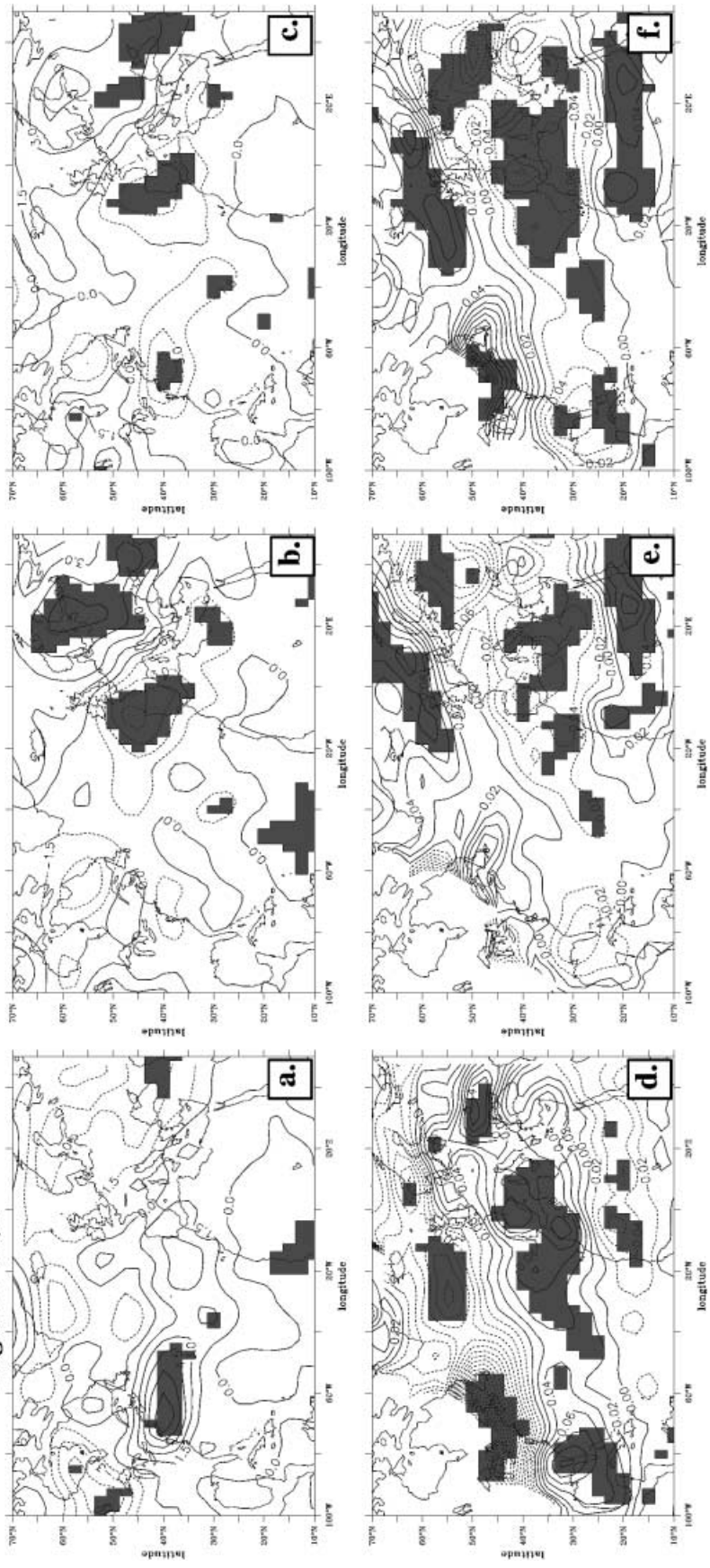

Fig. 5a-f Composites of STA (m) and σ_{BI} (day^{-1}) built on the SST index of Fig. 3: **a** negative and **b** positive composites of DJF STA, **c** weighted difference between the positive and negative composites of DJF STA. **d–f** same as **a–c** but for DJF σ_{BI}. Statistically significant regions according to a *t* test at the 95% level are shaded

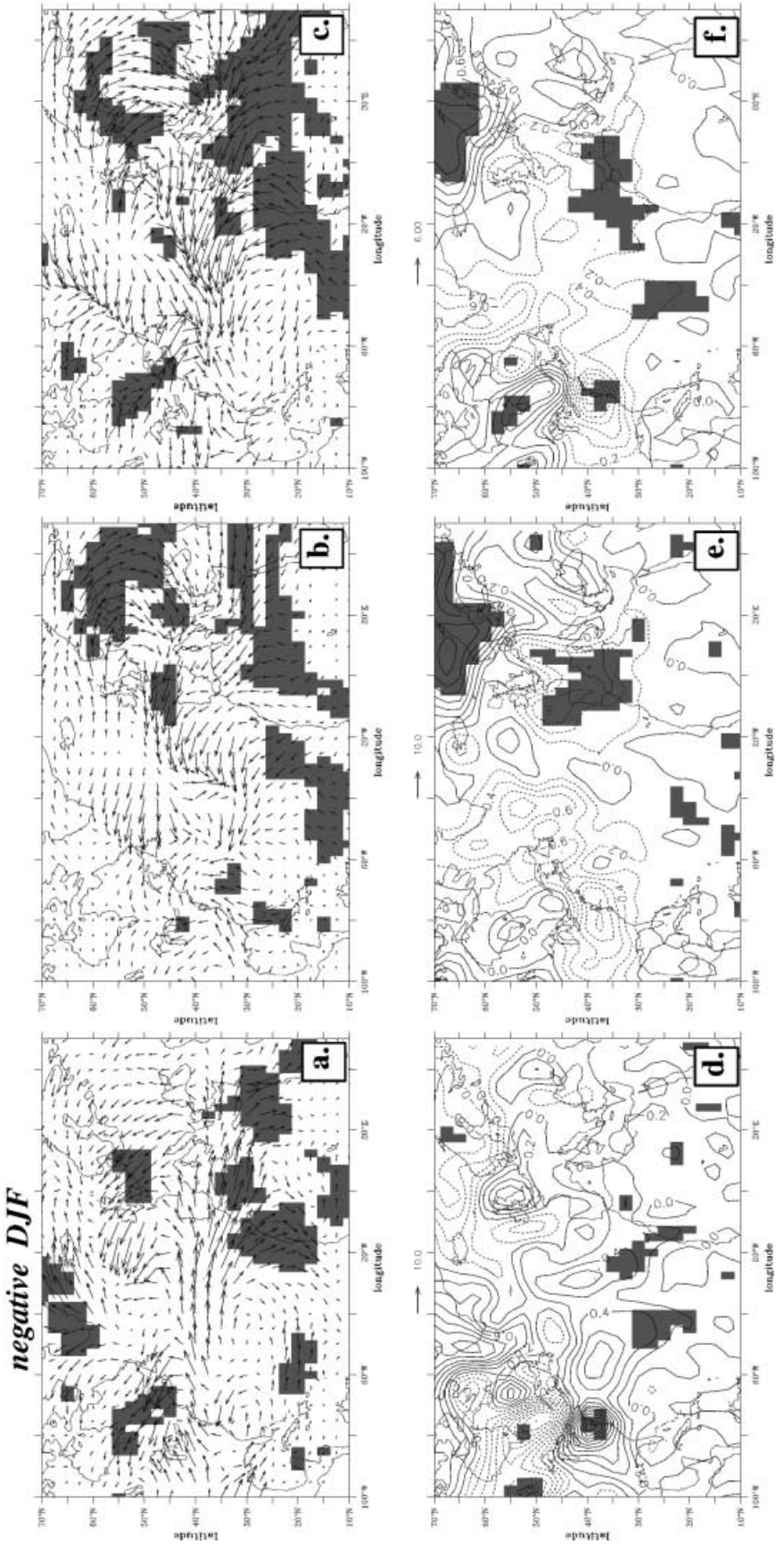

Fig. 6a–f Composites of **E** ($m^2.s^{-2}$) and $\overline{v'T'}$ ($m.K.s^{-1}$) built on the SST index of Fig. 3, as in Fig. 5. **a–c** for DJF **E** and **d–f** for DJF $\overline{v'T'}$

4.2 A mechanism involving stationary waves

As mentioned before, Fraedrich et al. (1993) found an atmospheric winter variability mode very similar to the Z500 anticyclonic anomaly. Composites of STA and **E** based on an index built on their atmospheric mode described above also display structures similar to those shown in Sect. 4.1. These composites suggest that the storm track acts as a positive feedback on the Z500 anomaly. If an anomalous stationary wave can initiate the Z500 anomaly, this eddy activity is likely to strengthen and maintain it in winter.

In Fig. 7, negative (positive) composites of 500 hpa geopotential height deviations from the zonal mean z^*, describe the stationary wave associated with a cold (warm) phase of the SST anomaly in DJF. The SST index (Fig. 3) is unchanged from Sect. 4.1. The negative composites show an elongated cyclonic anomaly extending throughout the North Atlantic basin and reaching Europe, associated with an anticyclonic structure centred above Eastern Europe and reaching Greenland to the west. This structure is likely to induce an anomalous zonal flow from Florida to the Gibraltar Straight, and decreased westerlies over Northern Europe. The difference between the positive and negative composites shows the significant NAO-like response to the summer SST anomaly. The anticyclonic anomaly amplitude is 40 m while the DJF anticyclonic structure covarying with the warm ASO SST anomaly initially found in the SVD A results was reaching 25 m (Fig. 2a).

In order to describe more precisely the response to the SST anomaly in terms of stationary wave activity, composites of the Plumb vector **F** are also displayed in Fig. 7. The negative composite shows a reduced stationary wave activity source located over the North Atlantic basin. A significant increase of stationary wave activity is found over the North Atlantic basin in the positive composite and in the difference, that is likely to induce the anticyclonic anomaly over Europe found in the wave train of the positive composite of z^*. The lagged composites of z^* and **F** built on SST SVD scores, give results that closely resemble those of Fraedrich et al. (1993). Their composites, however, were built on an atmospheric index representing the year to year fluctuations of the principal mode of winter climate variability in Europe. These similarities between those two composite analyses suggest that the SST anomaly can excite winter European climate into one of its main variability modes. The negative and positive composites of SST in DJF (not shown) are quasi-symmetrical and display the main features of the summer SST pattern of Fig. 2a, the central part of the anomaly being slightly shifted to the east. It is worth noting that in the positive composite, the central (midlatitude) warm anomaly is the most significant part of the SST anomaly, whereas in the negative it is the warm subtropical part.

If the area of interest is restricted to the European region for the atmosphere, the Z500 response to the summer SST anomaly is quasi-symmetrical, as can be seen in Fig. 7a, b, whereas in terms of STA it is asymmetrical (Fig. 5a, b). This might explain the non-significance of the results of the lead-lag SVD analysis SVD A between SST and STA despite the coherent spatial structures obtained (not shown). Thus, the atmospheric response to the summer SST anomaly appears to be non-linear. The assumption can be made that the warm phases of the persisting summer SST anomaly can trigger an anomalous stationary wave able to initiate a small atmospheric anticyclonic anomaly over Europe at the beginning of winter, since earlier lagged composites are not significant (not shown). The winter eddy activity linked to this warm phase lies in a northward shift of the tail end of the Atlantic storm track, consistent with the previously induced anticyclone, and allowing to drive and enhance it.

Hence we have shown the link between each component of the Fraedrich mechanism and the North Atlantic summer SST anomaly. Therefore the latter is found to be a possible triggering phenomenon for this mechanism. In the case of cold phases of the summer SST anomaly, the atmospheric variability mode excited is more zonally oriented and gives a significant response in fall (not shown). The latter is extending through the entire NAE region and not only over Europe as found in the warm phase counterpart.

5 Discussion

We have shown that a significant link exists in NCEP between a summer North Atlantic SST anomaly and the following winter atmospheric circulation over Europe. The summer SST anomaly, obtained by lead-lag SVD analysis between North Atlantic SST and Z500 over Europe (SVD A), is close to the first variability mode of North Atlantic SST for summer and fall seasons and persists until winter. The winter atmospheric spatial structure resembles the NAO but is more Europe-centred, thus closer to the pressure pattern of the first combined EOF of SLP, temperature and precipitations (Fraedrich et al. 1993).

Composites of different atmospheric circulation diagnostics, built on SST SVD A scores, emphasize the non-linearity of the atmospheric response to the sign of the SST anomaly. On one hand, a warm phase of the SST anomaly leads to the strengthening of STA over Northern Europe the next winter. This anomalous activity, through convergence of eddy vorticity flux onto the mean circulation, can lead to the growth and maintenance of an initially small anticyclonic anomaly over Europe. The warm anomaly is also linked to the occurrence of a stationary wave anomaly that could generate the anticyclonic anomaly over Europe, in agreement with the mechanism proposed by Fraedrich et al. (1993). On the other hand a cold phase of the SST anomaly is linked to a negative phase of the NAO pattern which is the major atmospheric variability mode throughout the year. STA enhancement over the sub-

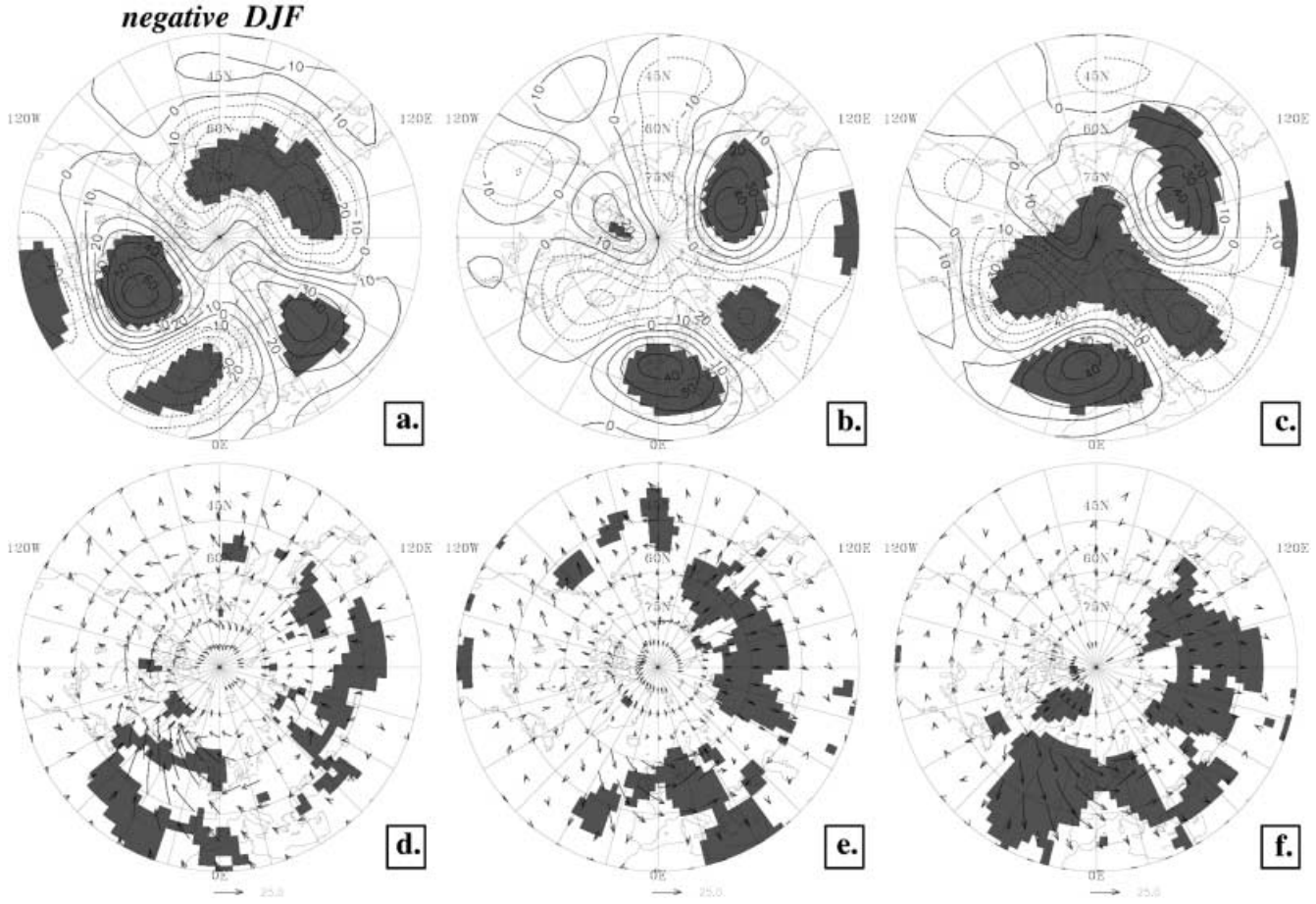

Fig. 7a–f Composites of z^* (m) and **F** ($m^2.s^{-2}$) built on the SST index of Fig. 3, as in Fig. 5. **a–c** for DJF z^* and **d–f** for DJF **F**

tropical North Atlantic ocean and towards the Bay of Biscay is significantly linked to this SST anomaly. The monthly composites of SLP built on a SST index in the 40°N–50°N, 60°W–40°W region by Peng and Fyfe (1996) show the relationship between a warm phase of an early winter SST anomaly close to the summer SST pattern we found, and a strong SLP anticyclonic monopole over the North Atlantic ocean basin in November. A recent study by Watanabe and Kimoto (2000) shows the role of a winter SST anomaly close to this summer pattern in forcing the winter atmospheric low frequency circulation. They detect this anomaly through combined SVD analysis between DJF SST forcing and response fields and Z500. They show its importance with the results of numerical experiments, coupling an oceanic boundary layer with a global atmospheric general circulation model (AGCM), with prescribed SST in the tropical band.

Fraedrich et al. (1993) suggest that such a mechanism is embedded in a global El Niño Southern Oscillation (ENSO) related climate fluctuation. As reviewed by Trenberth et al. (1998), the NAE atmospheric variability might be linked to ENSO through the excitation of the Pacific North America (PNA) pattern. This wave train affects the entire North American continent, with deepened Aleutian low, anomalous high over the northern sector, and a cyclonic anomaly over the southeast North American coasts. The atmospheric bridge theory (Lau and Nath 1994, 1996) suggests that the PNA induces in winter a warm subtropical Atlantic SST anomaly during El Niño years (warm SST along the Equator in the Pacific), associated with a negative phase of the NAO. On the negative composite of the Plumb vector **F** in OND (not shown) a significant wave propagation appears, crossing the North American continent, suggesting a Pacific/Atlantic connection. The anomalous Rossby wave propagation matching the PNA pattern during the El Niño years, resembles the corresponding wave propagation composite. This suggests that the cold phase of the summer SST anomaly is correlated to El Niño phases of ENSO and negative phases of the NAO. The Atlantic storm track is likely to maintain this pattern over the NAE region, as shown in Figs. 5 and 6. The splitting of the anticyclonic anomaly on the SVD Z500 pattern of Fig. 2a into an eastern part, and a western part located over one of the PNA centres of action also suggests an ENSO connection. The NAE region might be more sensitive to La Niña events as suggested by Chen (1982) and confirmed by Cassou

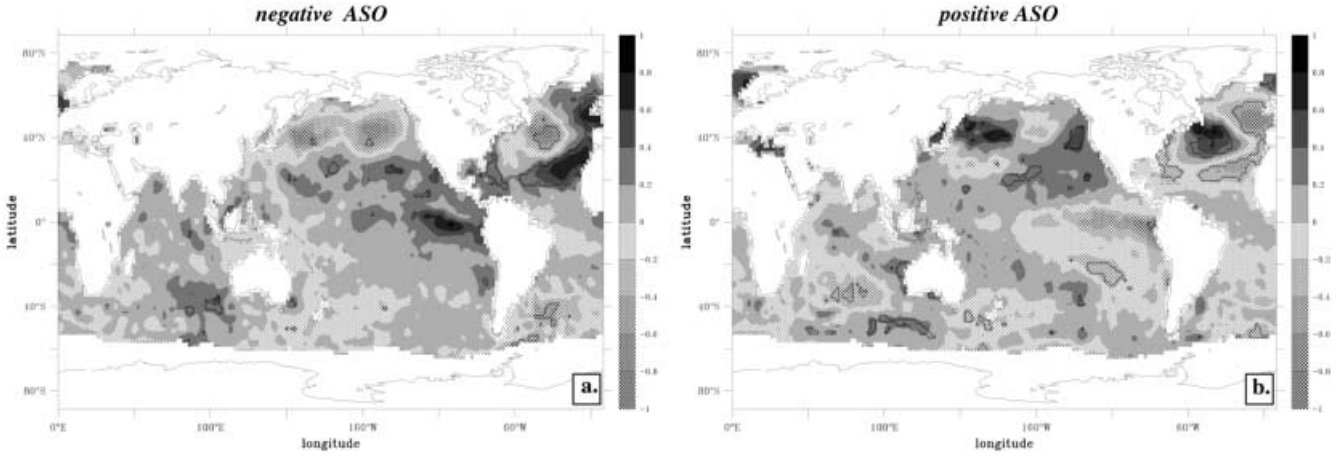

Fig. 8a, b Composites of SST (°C) built on the SST index of Fig. 3, **a** negative and **b** positive composites of ASO SST. The *thick lines* indicate statistically significant regions according to a *t* test at the 95% level

and Terray (2001). The extreme positive events of the SST SVD scores (Fig. 3) correspond in part to La Niña years, but composites of global summer SST do not significantly link cold SST anomalies in the tropical Pacific with the warm phase of the North Atlantic SST anomaly (Fig. 8b), nor does El Niño significantly influence cold phases (Fig. 8a), as the SST anomaly appears in summer and the El Niño SST anomalies in the Pacific reach their maximum in winter. The atmospheric bridge cannot generate the summer North Atlantic SST anomaly as the PNA is a winter variability mode.

The ENSO influence over Europe thus may be in addition to the ability of the summer North Atlantic SST anomaly to excite a European winter atmospheric variability mode. The non-linearity of the atmospheric response, either to tropical or extratropical SST, can be due to the dependence of the storm track location on the low frequency atmospheric fluctuations, leading to regional transient eddy feedbacks.

However, this statistical study is a preliminary investigation of the interactions between SST, low frequency circulation and the storm track in the NAE region. These first findings will help us to design further AGCM studies, first with prescribed SST anomalies, second coupled with a seasonally dependent oceanic boundary layer and finally with a realistic ocean. These sensitivity experiments will address the question of which physical mechanisms allow the SST to feedback on the mean flow or the storm track, leading to these observed statistical links. The coupled experiments will give some clues to the part played by the ocean in the occurrence of these summer SST anomalies.

Acknowledgements The NCEP/NCAR reanalysis data was provided for this study by the NOAA Climate Diagnostic Center. We thank the anonymous reviewers for their help in improving this manuscript. We also wish to thank Jean-Pierre Céron and Jean-François Guérémy for the Murakami filter program, Masa Kageyama for valuable comments and Sophie Valcke for helpful discussions and for her help in handling the data.

References

Barnston AG, Livezey RE (1987) Classification, seasonality and persistence of low-frequency atmospheric circulation patterns. Mon Weather Rev 115: 1083–1126

Blackmon ML (1976) A climatological spectral study of the 500 mb geopotential height of the northern hemisphere. J Atmos Sci 33: 1607–1623

Blender R, Fraedrich K, Lunkeit F (1997) Identification of cyclone-track regimes in the North Atlantic. Q J R Meteorol Soc 123: 727–741

Branstator G (1995) Organization of storm track anomalies by recurring low frequency circulation anomalies. J Atmos Sci 52: 207–226

Bresch DN, Davies HC (2000) Covariation of the mid-tropospheric flow and the sea surface temperature of the North Atlantic: a statistical analysis. Theoret Appl Climat 65: 197–214

Bretherton CS, Smith C, Wallace JM (1992) An intercomparison of methods for finding coupled patterns in climate data. J Clim 5: 541–560

Cassou C, Terray L (2001) Dual influence of Atlantic and Pacific SST anomalies on the North Atlantic/Europe winter climate. Geophys Res Lett (in press)

Chen WY (1982) Fluctuations in northern hemisphere 700 mb height field associated with the Southern Oscillation. Mon Weather Rev 110: 808–823

Christoph M, Ulbrich U, Haak U (1995) Faster determination of the intraseasonal variability of storm tracks using Murakami's recursive filter. Mon Weather Rev 123: 578–581

Czaja A, Frankignoul C (1999) Influence of the North Atlantic SST on the atmospheric circulation. Geophys Res Lett 26: 2969–2972

da Silva A, Young C (1994) Atlas of surface marine data. US. Department of Commerce, National Oceanic and Atmospheric Administration, Washington, DC, USA

Fraedrich K, Bantzer C, Burkhardt U (1993) Winter climate anomalies in Europe and their associated circulation at 500 hpa. Clim Dyn 8: 161–175

Frankignoul C (1985) Sea surface temperature anomalies, planetary waves, and air-sea feedback in the middle latitudes. Rev Geophys 23: 357–390

Frankignoul C, Müller P, Zorita E (1997) A simple model of the decadal response of the ocean to stochastic wind forcing. J Phys Oceanogr 27: 1533–1546

Hoskins BJ (1983) Modelling of the transient eddies and their feedback on the mean flow. In: Hoskins BJ, Pearce RP (eds), Large-scale dynamical processes in the atmosphere, Academic Press, New York, pp 169–199

Hoskins BJ, Valdes PJ (1990) On the existence of storm-tracks. J Atmos Sci 47: 1854–1864

Iwasaka N, Wallace JM (1995) Large scale air sea interaction in the Northern Hemisphere from a view point of variations of surface heat flux by SVD analysis. J Meteorol Soc Japan 73: 781–794

Kalnay E and Coauthors (1996) The NCEP/NCAR 40-year reanalysis project. Bull Am Meteorol Soc 77: 437–472

Kushnir Y (1994) Interdecadal variations in North Atlantic sea surface temperature and associated atmospheric conditions. J Clim 7: 141–157

Lau N-C (1988) Variability of the observed midlatitude storm tracks in relation to low-frequency changes in the circulation pattern. J Atmos Sci 45: 2718–2743

Lau N-C, Nath MJ (1994) A modelling study of the relative roles of tropical and extratropical SST anomalies in the variability of the global atmosphere-ocean system. J Clim 7: 1184–1207

Lau N-C, Nath MJ (1996) The role of the "atmospheric bridge" in linking tropical pacific ENSO events to extratropical SST anomalies. J Clim 9: 2036–2056

Lindzen RS, Farrel B (1980) A simple approximate result for the maximum growth rate of baroclinic instabilities. J Atmos Sci 37: 1648–1654

Norris JR (2000) Interannual to interdecadal variability in the storm track, cloudiness, and sea surface temperature over the summertime North Pacific. J Clim 13: 422–430

Peng S, Fyfe J (1996) The coupled patterns between sea level pressure and sea surface temperature in the midlatitude North Atlantic. J Clim 9: 1824–1839

Peng S, Whitaker JS (1999) Mechanisms determining the atmospheric response to midlatitude SST anomalies. J Clim 12: 1393–1408

Peng S, Mysak LA, Ritchie H, Derome J, Dugas B (1995) The differences between early and midwinter responses to sea surface temperature anomalies in the northwest Atlantic. J Clim 8: 137–157

Plumb RA (1985) On the three-dimensional propagation of stationary waves. J Atmos Sci 42: 217–229

Rogers JC (1990) Patterns of low frequency sea level pressure variability (1899–1986) and associated wave cyclone frequencies. J Clim 3: 1364–1379

Rogers JC (1997) North Atlantic variability and its association to the North Atlantic Oscillation and climate variability of Northern Europe. J Clim 10: 1635–1647

Sciremammano Jr F (1979) A suggestion for the presentation of correlations and their significance levels. J Phys Oceanogr 9: 1273–1276

Schubert M, Perlwitz J, Blender R, Fraedrich K, Lunkeit F (1998) North Atlantic cyclones in CO_2-induced warm climate simulations: frequency, intensity, and tracks. Clim Dyn 14: 827–837

Trenberth KE (1986) An assessment of the impact of transient eddies on the zonal flow during a blocking episode using localized Eliassen-Palm flux diagnostics. J Atmos Sci 43: 2070–2087

Trenberth KE, Branstator GW, Karoly D, Kumar A, Lau N-C, Ropelewski C (1998) Progress during TOGA in understanding and modeling global teleconnections associated with tropical sea surface temperatures. J Geophys Res 103: 14291–14324

Ulbrich U, Christoph M (1999) A shift of the NAO and increasing storm track activity over Europe due to anthropogenic greenhouse gas forcing. Clim Dyn 15: 551–559

Wallace JM, Smith C, Bretherton CS (1992) Singular value decomposition of wintertime sea surface temperature and 500-mb height anomalies. J Clim 5: 561–576

Watanabe M, Kimoto M (2000) Atmosphere-ocean thermal coupling in the North Atlantic: a positive feedback. Q J R Meteorol Soc 126: 3343–3369

Wilks DS (1997) Resampling hypothesis tests for autocorrelated fields. J Clim 10: 65–82

Zhang Y, Norris JR, Wallace JM (1998) Seasonality of large-scale atmosphere-ocean interaction over the north pacific. J Clim 11: 2473–2481